

Sensor Selection and Power Allocation for Distributed Estimation in Sensor Networks: Beyond the Star Topology

Gautam Thatte, *Student Member, IEEE*, and Urbashi Mitra, *Fellow, IEEE*

Abstract—Optimal power allocation for distributed parameter estimation in a wireless sensor network with a fusion center under a total network power constraint is considered. For the simple star topology, an analysis of the effect of the measurement noise variance on the optimal power allocation policy is presented. The optimal solution evolves from sensor selection, to water-filling, to channel inversion as the measurement noise variance increases; in the last solution, the sensor with the weakest channel signal-to-noise ratio (SNR) is allocated the largest fraction of the total power. Relaying nodes are then introduced to form the more complex branch, tree, and linear topologies. The optimal power allocation strategies for these complex topologies are then considered for both amplify-and-forward and estimate-and-forward transmission protocols. Analytical solutions for these cases appear to be intractable, and thus asymptotically optimal (for increasing measurement noise variance) solutions are derived. The solutions to this asymptotic problem offer near-optimal performance even for modest measurement noise. The optimal limiting power policy for the leaf nodes in branch and tree topologies is channel inversion, whereas in linear networks, the optimal solution is a form of weighted channel inversion. The results are extended to a multipath channel model and to the estimation of a vector of random parameters.

Index Terms—Multisensor systems, parameter estimation, resource management.

I. INTRODUCTION

WIRELESS SENSOR NETWORKS (WSNs) have garnered recent interest due to their potential for sensing the physical world. In contrast to classical networks, WSNs have strict limitations on resources such as energy, bandwidth, and computational complexity, but are deployed in very high densities. Since limited power resources represent a challenge for the design and implementation of WSNs, consideration of performance per a power constraint and power minimization per a performance constraint are approaches of interest. In this paper, we study the problem of optimal power allocation given a total network transmit power constraint with the goal of minimizing the mean-squared error (MSE) for a parameter

estimation problem. Motivated by [1], which suggests that communication power consumption accounts for 70% of the total power in a sensor network, our work focuses on optimizing the power used to communicate measurements rather than considering resources used for sensing and signal processing.

Due to the anticipated applications of WSNs, there has been significant activity in the areas of distributed estimation and detection. For example, scalar parameter estimation [2]–[8] and spatial field estimation [9] based on minimizing the mean-squared error have been previously considered. Examples of deployed sensor networks sensing scalar parameters, e.g., the surface temperature of a lake, and transmitting measurements to a leader node include [10]–[12]. Maximum likelihood estimation of a correlated Gaussian source, as in [13], relies on explicit knowledge of the underlying statistics of the phenomenon to be sensed.

Distributed estimation is realized in one of two ways: either using decentralized schemes, as in [2], or in a centralized framework with a fusion center or leader node, as in [14]. In the latter, a leader node iterates over all as yet unincorporated sensors and chooses among them in order to maximize a utility functional. For the type of distributed estimation problem we consider, the MSE functional captures both the utility of the nodes and the measurement quality. Both a similar problem to what is considered here and the “dual” of that problem (power minimization to meet an MSE criterion) were considered in [3] and [4] respectively for the simple star topology.

In contrast to [13], the linear MMSE-based approaches considered in our work only require second order statistics, and no other knowledge of the underlying distributions, with some subsequent potential loss of performance. We focus on a particular instantiation of a WSN topology wherein a fusion center receives noisy measurements¹ from a number of geographically distributed sensors, as shown in Fig. 1(a)–(c) for different topologies. All sensors make measurements, but some also act as relay nodes that forward information to the fusion center. We assume that the fusion center determines the optimal power allocation strategy to minimize the estimation error, and that this optimal strategy is conveyed, distortion-free, to the respective nodes. Our previous work [15] extended the parameter estimation problem to the branch and tree topologies for the case where relaying nodes do not have individual measurements. This work further considers measurements *at*

Manuscript received November 30, 2006; revised November 13, 2007. This work was supported in part by the National Science Foundation and by the Office of Naval Research by Grants ONR N-000140410273, NSF ITR CCF-0313392, and NSF OCE 0520324. The associate editor coordinating the review of this manuscript and approving it for publication was Dr. Thierry Blu.

The authors are with the Communication Sciences Institute, Ming Hsieh Department of Electrical Engineering, University of Southern California, Los Angeles, CA 90089 USA (e-mail: thatte@usc.edu; ubli@usc.edu).

Digital Object Identifier 10.1109/TSP.2008.917038

¹Our work focuses on an analog transmission of measurements to the fusion center. We refer the reader to [3], [7] and [8] for the effect of quantization on the optimization problem.

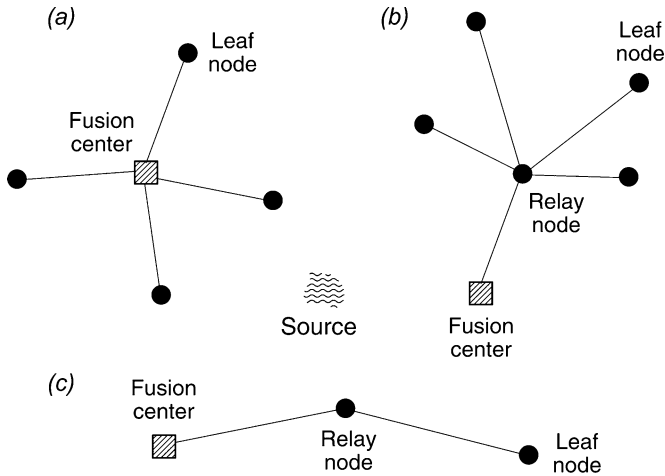


Fig. 1. Sensor network (a) star; (b) branch; and (c) linear topologies.

all nodes, and develops strategies for optimal power allocation for the branch, tree, and linear topologies with relaying nodes. The main contributions of this paper are as follows.

- It extends the work of [4], which provides the optimal solution to the gain allocation problem. The power allocation strategy for the simple star topology is derived and characterized for different ranges of the measurement noise variance.
- The more complex multihop linear, branch, and tree topologies are examined and appear to have intractable analytic solutions. Therefore, asymptotically optimal solutions for increasing measurement noise variance are derived for both amplify-and-forward and estimate-and-forward protocols. It is observed that the solutions to the limiting problem offer near-optimal performance even for modest measurement noise.
- The tradeoff between channel quality and measurement quality is assessed; the optimal power policy evolves as a function of both these factors. For example, we find that sensor/branch selection is optimal for low measurement noise, but all sensors should remain active as measurement noise increases.

It must be noted that for the simple star topology, the optimal power allocation strategy in the low measurement noise variance case resembles the waterfilling² power allocation strategy for single-user multiple-input multiple-output (MIMO) channels [16]. On the other hand, the optimal solution for high measurement noise variance has no MIMO equivalent, and the complex topologies considered in this work cannot be meaningfully correlated to the theory of multiuser communications.

The remainder of this paper is organized as follows. Section II defines the signal models, topologies, and transmission protocols that are used throughout the paper. The optimal power allocation policy for the star topology is presented in Section III, along with the analysis that extends the work of [4] and [15]. Section IV develops the power allocation problem and asymptotic solution for the branch topology using both amplify-and-forward and estimate-and-forward protocols. The branch topology is extended to the tree topology in Sections V,

²The waterfilling power policy allocates more power to the sensor with the better channel SNR.

and VI develops the linear topology case. Numerical results comparing the estimate-and-forward and amplify-and-forward transmission protocols, as well as the different topologies, are presented in Section VII. Section VIII provides conclusions and future work. The appendices examine an argument for time-orthogonal communication, and extensions to multipath channels and vector parameter estimation, respectively.

II. SYSTEM AND NETWORK MODELS

A. System Model

A star topology with sensors directly connected to the fusion center is depicted in Fig. 1(a). Each of the N leaf nodes sends a noisy measurement of a deterministic function³ $f_i(\cdot)$ of the random zero-mean scalar parameter θ with variance $\sigma_\theta^2 < \infty$ to the fusion center; the received signal from the i th node is given by

$$y_i = \sqrt{P_i} h_i \beta(z_i) [f_i(\theta) + z_i] + n_i \quad i = 1, \dots, N \quad (1)$$

where P_i and h_i are the allocated transmission power and the nonrandom channel attenuation coefficient for node i , respectively. The noise terms z_i and n_i represent the zero-mean measurement noise with variance $\sigma_{z_i}^2$ and the channel noise with variance $\sigma_{n_i}^2$, respectively, both with unknown pdfs. We define the normalization factor⁴

$$\beta(z) = 1 / \sqrt{\sigma_{f_i(\theta)}^2 + \sigma_z^2} \quad (2)$$

for a generic noise term z , where $\sigma_{f_i(\theta)}^2$ is the variance of the deterministic function of the random scalar parameter θ to be estimated at the fusion center. The function $f_i(\theta)$ observed by the sensors could depend on the sensor-source distance, for example, but it is assumed *not* to be a function of the transmission power. Thus any deterministic function can be incorporated into our framework, but to simplify the notation and analysis, we simply consider the scalar parameter measurement for the remainder of our paper.

Note that the measurement noise z_i is defined generally; two main types are envisioned.

- 1) In one instance, measurement noise is interpreted as the quality of the measurement taken by a particular sensor. A sensor being closer to the source results in a lower measurement noise variance, and thus the measurement noise variances are topology-dependent.
- 2) In the other instance, the measurement noise variance represents the intrinsic error present due to hardware limitations in each sensor. In this case, the measurement noise variance is identical for all sensors.

We further assume that the channel and measurement noises are independent and that the channel gains are known at the fusion center via channel estimation algorithms using training sequences (see, for example, the work of Caire and Mitra [17]).

³The function of the scalar random variable $f_i(\theta)$ must have finite first and second moments, i.e., $\sigma_{f_i(\theta)}^2 < \infty$.

⁴This normalization factor is chosen to ensure that the transmitted signal from any node has unit variance. Thus the term P_i represents the physical power used to communicate the measurement.

Given the model assumptions, the optimal linear estimate that minimizes the mean-squared error is the best linear unbiased estimate (BLUE) [18].⁵ We denote $r_i = |h_i|^2/\sigma_{n_i}^2$ to be the effective channel SNR for the i th sensor. The optimization problem considered in this paper is minimizing the BLUE MSE subject to a total network power constraint $\sum_{\forall i} P_i = P_T$.

Note that the signal model in (1) assumes that measurements of the scalar parameter θ are transmitted time-orthogonally from the leaf nodes to the fusion center. This transmission scheme is proven to be optimal⁶ in the case of estimating a vector of parameters [19]. For orthogonal communication, in this scalar parameter estimation framework, [4] proves that the MSE does not approach zero as the number of sensors increases to infinity for a fixed total power, although systems based on nonorthogonal schemes can drive the MSE to zero. On the other hand, as the measurement noise variance increases, the MSE for the orthogonal scheme is lower than for the other extreme (the parallel transmission case), as shown in Appendix I. Thus, the orthogonal transmission scheme offers a good trade-off between performance, practical implementation, and tractability.

The more complex branch, tree, and linear topologies are considered in Sections IV–VI. Unlike the star topology, these topologies consist of both relay nodes and leaf nodes. The relay nodes make measurements, and also forward the leaf node measurements to the fusion center, thus necessitating the need for transmission protocols.

B. Relay Transmission Protocols

For the multihop topologies, we first define the amplify-and-forward (AF) scheme wherein the measurement from the leaf node is simply scaled and forwarded by the relay node. The second scheme is the estimate-and-forward (EF) protocol which estimates the parameter at the relay using the received measurement, and then transmits this new estimate onwards. For both relay protocols, the transmitted signal from any node is always normalized; thus P_i actually represents the physical power used to forward a measurement or estimate. Furthermore, in these topologies, time-orthogonal transmission is assumed within each level, e.g., leaf nodes to relay nodes and relay nodes to the fusion center in any generic two-hop topology.

For example, consider a simple two-hop linear network as shown in Fig. 1(c) with measurements made at both the leaf and

⁵If the measurement and channel noises are Gaussian, the BLU estimate is equivalent to the optimal MMSE estimate.

⁶The optimality of the transmission scheme in [19] is with respect to the sum distortion.

relay nodes. In the AF case, we assume that the power allocated to a relay node is divided equally between all the measurements that are forwarded through that relay.⁷ Using this protocol, the fusion center receives two measurements

$$y_1 = \sqrt{\frac{P_0}{2}} h_0 \gamma(P_1) [\sqrt{P_1} h_1 \beta(z_1) (\theta + z_1) + n_1] + n_{01} \quad (3)$$

$$y_2 = \sqrt{\frac{P_0}{2}} h_0 \beta(z_0) (\theta + z_0) + n_{02} \quad (4)$$

from the leaf node and relay node, respectively. We define another normalization function

$$\gamma(P_i) = 1 / \sqrt{P_i h_i^2 + \sigma_{n_i}^2} \quad (5)$$

for any power term P_i , and $\beta(z_i)$ is as defined in (2). Note that there is no estimation at the relay node because this node simply uses its allocated power, P_0 , to retransmit the signal, instead of processing it. The two measurements received at the fusion center are used to compute the BLU estimate with the corresponding estimation error given by

$$\text{MSE}_{\text{AF}} = \left(\frac{1}{\sigma_{z_0}^2 + \frac{2}{r_0 P_0 \beta^2(z_0)}} + \frac{1}{\sigma_{z_1}^2 + \frac{1}{r_1 P_1 \beta^2(z_1)} \left(1 + \frac{2}{r_0 P_0 \gamma^2(P_1)} \right)} \right)^{-1} \quad (6)$$

where r_0 and r_1 are the effective channel SNRs of the fusion center to relay node link and relay to leaf node link, respectively.

On the other hand, the estimate-and-forward protocol involves obtaining an estimate for the parameter at the relay. The two measurements received at the relay are given by

$$y_1 = \sqrt{P_1} h_1 \beta(z_1) (\theta + z_1) + n_1 \quad (7)$$

$$y_2 = \theta + z_0 \quad (8)$$

and the BLU estimate computed at the relay, denoted $\hat{\theta}_R$, is shown in (9) at the bottom of the page.

⁷An unequal division of relay node power is analogous to a different “branch” (see Section IV) with the same channel gain; thus assuming equal powers for all measurements transmitted from a relay node allows for a fair comparison between topologies.

$$\hat{\theta}_R = \theta + \underbrace{\left(\frac{1}{\sigma_{z_0}^2} + \frac{1}{\sigma_{z_1}^2 + \frac{1}{r_1 P_1 \beta^2(z_1)}} \right)^{-1}}_{w_0} \left(\frac{z_0}{\sigma_{z_0}^2} + \frac{P_1 h_1^2 \beta^2(z_1) z_1 + \sqrt{P_1} h_1 \beta(z_1) n_1}{P_1 h_1^2 \beta^2(z_1) \sigma_{z_1}^2 + \sigma_{n_1}^2} \right). \quad (9)$$

This single measurement $\theta + w_0$ is transmitted from the relay to the fusion center, which receives

$$y = \sqrt{P_0} h_0 \beta(w_0) \hat{\theta}_R + n_0. \quad (10)$$

The received measurement y is used to compute the final estimate at the fusion center, denoted $\hat{\theta}_{FC}$, as

$$\hat{\theta}_{FC} = \theta + w_0 + \frac{n_0}{P_0 h_0^2 \beta^2(w_0)} \quad (11)$$

with the corresponding MSE derived as

$$\text{MSE} = \frac{1}{r_0 P_0 \beta^2(w_0)} + \underbrace{\left(\frac{1}{\sigma_{z_0}^2} + \frac{1}{\sigma_{z_1}^2 + \frac{1}{r_1 P_1 \beta^2(z_1)}} \right)^{-1}}_{\sigma_{w_0}^2}. \quad (12)$$

Although the signal models and MSE expressions are derived for the simple two-hop network, the two protocols remain the same for multihop networks. The communication power allocated to a relaying node is divided equally between all the measurements that must be transmitted through that node. A key difference between the AF and EF protocols is the fact that in the former, the noise in each link is propagated through the system, whereas in the latter, the estimation error from each relay is transmitted through the network.

III. THE STAR TOPOLOGY

A. Optimal Power Allocation and Sensor Selection

Recall the signal model for the star topology from (1). The MSE corresponding to the BLU estimate formed at the fusion center is given by

$$\text{MSE}_{\text{star}} = \left(\sum_{i=1}^N \frac{1}{\sigma_{z_i}^2 + \frac{\sigma_\theta^2 + \sigma_{z_i}^2}{r_i P_i}} \right)^{-1}. \quad (13)$$

To minimize the MSE of the parameter estimate obtained at the fusion center subject to a total network power constraint, the following optimization problem is considered:

$$\begin{aligned} \min_{\mathbf{P}} \text{MSE}_{\text{star}} \quad & \text{subject to } \sum_{i=1}^N P_i = P_T \\ & \text{and } -P_i \leq 0, \quad i = 1, \dots, N \end{aligned} \quad (14)$$

where $\mathbf{P} = (P_1, P_2, \dots, P_N)$ are the powers allocated to the N nodes. We use Lagrange multiplier theory to solve the optimization problem since the MSE is a convex function in \mathbf{P} (as done independently in [4] for gain optimization). Define ν and $\lambda = (\lambda_1, \lambda_2, \dots, \lambda_N)$ as the Lagrange multipliers associated with the equality total network power constraint and the inequality constraints, respectively. The solutions derived for the

star topology, as well as for the branch, tree, and linear topologies in the later sections, are globally optimal and unique since the MSE functionals for all the topologies are convex. We can prove convexity using the positive-definiteness of the Hessian matrix, and the results of [20] as follows.

- 1) If $f(x)$ is positive and convex (concave), then $1/f(x)$ is concave (convex).
- 2) Weighted nonnegative sums of concave (convex) functions are necessarily concave (convex).

Given that both the objective function and the power constraint are convex, the Karush-Kuhn-Tucker conditions are valid [20]. The optimal solution is derived as

$$P_i^* = \begin{cases} \frac{\sigma_\theta^2 + \sigma_{z_i}^2}{r_i \sigma_{z_i}^2} \left(\sqrt{\frac{r_i}{\nu^* (\sigma_\theta^2 + \sigma_{z_i}^2)}} - 1 \right) & \text{if } \lambda_i^* = 0 \\ 0 & \text{if } \lambda_i^* = \nu^* - \frac{r_i}{\sigma_\theta^2 + \sigma_{z_i}^2}. \end{cases} \quad (15)$$

This solution suggests that some sensors should remain inactive in order to minimize the estimation MSE. Once the number of active sensors has been determined, (15) gives the optimal power allocated to each of the active sensors.

The number of active sensors $N' \leq N$ is the greatest integer that satisfies the inequality

$$\begin{aligned} \sqrt{\nu^*} &= \sum_{i=1}^{N'} \frac{1}{\sigma_{z_i}^2} \sqrt{\frac{\sigma_\theta^2 + \sigma_{z_i}^2}{r_i}} \bigg/ \left(P_T + \sum_{i=1}^{N'} \frac{\sigma_\theta^2 + \sigma_{z_i}^2}{r_i \sigma_{z_i}^2} \right) \\ &< \sqrt{\frac{r_{N'}}{\sigma_\theta^2 + \sigma_{z_{N'}}^2}} \end{aligned} \quad (16)$$

and the optimal power allocated to each of the sensors is computed as

$$P_i^* = \frac{\sigma_\theta^2 + \sigma_{z_i}^2}{r_i \sigma_{z_i}^2} \left(\sqrt{\frac{r_i}{\nu^* (\sigma_\theta^2 + \sigma_{z_i}^2)}} - 1 \right)^+, \quad \forall i \quad (17)$$

where $(x)^+$ equals 0 when $x < 0$, and is otherwise equal to x .

B. Analysis and Asymptotic Results

We first consider the case where $\sigma_{z_i}^2 = 0 \forall i$ —we have noiseless measurements. In this case, the optimization problem is stated as

$$\begin{aligned} \text{minimize } & \sigma_\theta^2 \left(\sum_{i=1}^N r_i P_i \right)^{-1} \quad \text{subject to } \sum_{i=1}^N P_i = P_T \end{aligned} \quad (18)$$

and the optimal solution would be to allocate all the power to the sensor(s) with the highest (common) SNR, yielding a sensor selection solution.⁸

Prop: Given M sensors with the same maximum SNR, $r_{\max} = r_1 = \dots = r_M$, and $N - M$ sensors with lower SNRs, $r_{\max} > r_{M+1} \geq \dots \geq r_N$, the power strategy that optimizes (18) is arbitrary allocation of the total power P_T amongst these M sensors.

⁸For multiple sensors with the same maximum SNR, any arbitrary power allocation amongst those sensors is optimal.

Proof: Consider two distinct power allocation schemes

$$\mathbf{P}^* = (\hat{P}_1, \hat{P}_2, \dots, \hat{P}_M, 0, \dots, 0)$$

and $\mathbf{P}_B = (P_1, P_2, \dots, P_M, P_{M+1}, \dots, P_N)$

where \mathbf{P}^* arbitrarily allocates power only to the subset of M sensors with the maximum SNR. The scheme \mathbf{P}_B also requires $P_i \geq 0$ for $i = M + 1, \dots, N$, which results in power being allocated to weaker SNR sensors. The MSE for the power allocation strategies can be computed as

$$\text{MSE}(\mathbf{P}^*) = \frac{\sigma_\theta^2}{r_{\max} P_T}$$

and $\text{MSE}(\mathbf{P}_B) = \frac{\sigma_\theta^2}{r_{\max} P_T - \Delta P}$

where $\Delta P = (r_{\max} - r_{M+1})P_{M+1} + \dots + (r_{\max} - r_N)P_N > 0$ since $P_i > 0$ for $i > M$. This implies $\text{MSE}(\mathbf{P}^*) < \text{MSE}(\mathbf{P}_B)$, and concludes the proof. ■

Since only “perfect” measurements of the *same* scalar parameter are transmitted by all the sensors, this optimal strategy is intuitive because all the power is allocated to the sensor(s) with the best channel SNR to ensure that the measurement is received with minimum distortion (due to channel noise) at the fusion center. We observe that the optimal solution described in (17) is a type of waterfilling solution [20] for low measurement noise variance. The $\sigma_{z_i}^2 = 0 \forall i$ case is an example of extreme waterfilling wherein the sensor with the maximum SNR is allocated all the power. As the measurement noise variance increases, waterfilling is *not* optimal. The optimal power allocation policy evolves to channel inversion.⁹

To facilitate analysis and the development of intuition, let the measurement noise variance of all the sensors be equal, $\sigma_{z_i}^2 = \sigma_z^2 \forall i$. Now consider the case of $\sigma_z^2 \rightarrow \infty$, i.e., all the available measurements get noisier. Note that for $\sigma_z^2 \approx 0$, only the sensor with the best SNR is active; as the measurement noise variance increases, other sensors become active. A method to analytically compute the threshold $\sigma_{z_i}^2$ at which each of the sensors becomes active is enumerated below. Without loss of generality, assume $r_1 > r_2 > \dots > r_N$ so that the N th sensor becomes active when the measurement noise variance is $\sigma_{z(N)}^2$.

- 1) Rewrite $\text{MSE} = f(P_1, \dots, P_N)$ using $P_N = 1 - \sum_{i=1}^{N-1} P_i$ as $\text{MSE} = g(P_1, \dots, P_{N-1})$.
- 2) Compute the quantity $(\partial g / \partial P_i)$ for $i = 1, 2, \dots, N - 1$, and solve the $N - 1$ equations

$$\frac{\partial g}{\partial P_i} = 0, \quad i = 1, 2, \dots, N - 1$$

to obtain the optimal allocation $\{P_1^*, P_2^*, \dots, P_{N-1}^*\}$.

- 3) Find the threshold $\sigma_{z(N)}^2$ that satisfies the equation $P_1^* + P_2^* + \dots + P_{N-1}^* = 1$.

The optimal allocated powers for the $N = 2, 3$ sensor cases as a function of equal measurement noise variance are shown in Fig. 2, represented by the bold and regular lines, respectively.

⁹The optimal limiting power allocation policy $\bar{\mathbf{P}}^*$ is termed channel inversion (or power equalization in [21]), which is defined as allocating the greatest fraction of the total power to the node with the weakest channel SNR.

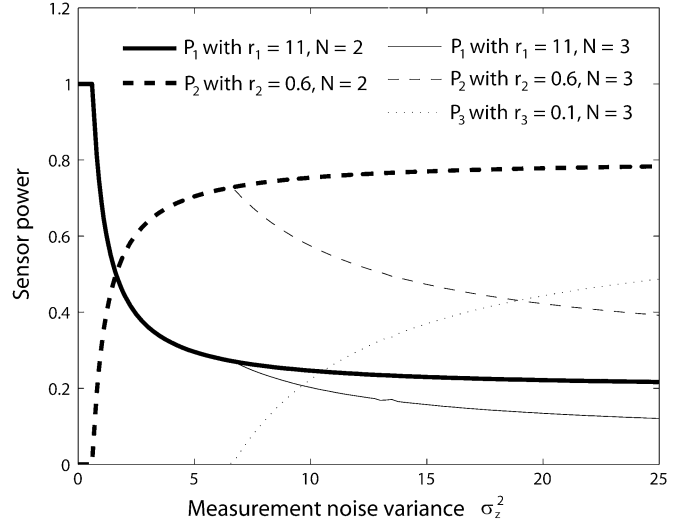


Fig. 2. Optimal power allocation for increasing σ_z^2 for $N = 2, 3$ star topology.

We see that for $\sigma_z^2 = 0$, all the power is allocated to the sensor with the maximum SNR ($r_1 = 11$), as predicted by Proposition 1. As the measurement noise variance increases, the remaining sensors are activated in order of descending channel SNRs. In the $N = 3$ sensor case, when the sensor with the weakest SNR is inactive, the optimal power allocation $\{P_1^*, P_2^*\}$ is the same as that for the $N = 2$ sensor case. When $\sigma_z^2 > 20$, the optimal solution has evolved to channel inversion (from waterfilling), wherein the weakest sensor ($r_3 = 0.1$) is allocated the greatest fraction of the total power. The threshold $\sigma_{z(3)}^2$ at which the third sensor becomes active can be computed using the algorithm described above. Since the fusion center has perfect channel state information, it can perform these computations in the N sensor case to determine which sensors should be activated as the measurement noise variance increases.

Notice that for large σ_z^2 , all the sensors are active; we denote the optimal limiting power allocation as $\{\bar{P}_i^*\}_{i=1}^N$. For all active sensors, (17) can be simplified to

$$P_i^* = \frac{1/\sqrt{r_i}}{\sum_{j=1}^{N'} 1/\sqrt{r_j}} P_T + \left(\frac{\sigma_\theta^2 + \sigma_z^2}{\sigma_z^2} \right) \times \left[\frac{1/\sqrt{r_i}}{\sum_{j=1}^{N'} 1/\sqrt{r_j}} \sum_{j=1}^{N'} \frac{1}{r_j} - \frac{1}{r_i} \right]. \quad (19)$$

Now we can explicitly compute the limiting optimal power for the nodes in the star topology as

$$\bar{P}_i^* = \lim_{\sigma_z^2 \rightarrow \infty} P_i^* = \frac{\alpha}{\sqrt{r_i}} \left(P_T + \sum_{j=1}^N \frac{1}{r_j} \right) - \frac{1}{r_i}$$

where $\alpha = \left(\sum_{j=1}^N \frac{1}{\sqrt{r_j}} \right)^{-1}$. (20)

The form of the optimal limiting solution $\bar{\mathbf{P}}^*$ is termed channel inversion. Since the optimal power P_i is proportional to $r_i^{-\gamma}$ (for some $\gamma > 0$), the sensor with the highest SNR is allocated the smallest fraction of the total power.

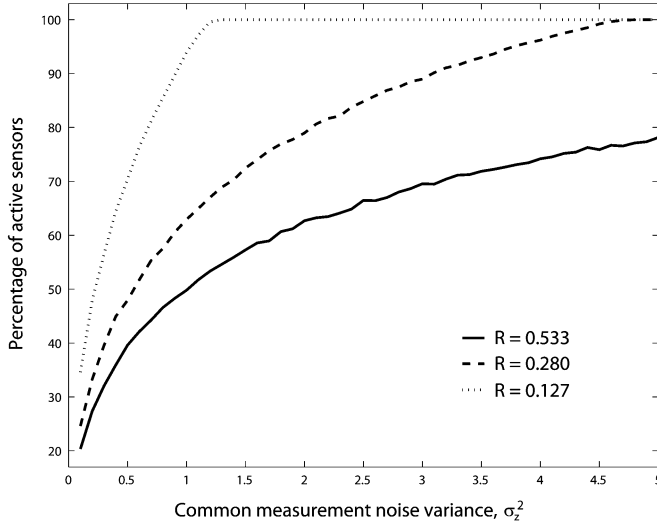


Fig. 3. Percentage of active sensors versus increasing σ_z^2 for different \tilde{R} .

The evolution of the optimal power allocation scheme from sensor selection and waterfilling to channel inversion is similar (in the extreme cases) to the mercury/waterfilling solution derived in [21], where mutual information in parallel channels is maximized. The asymptotic behavior is with respect to the total available power in [21], and measurement noise variance in our work. Note that the optimal power allocation strategy is unaffected by the total power available in the case of high measurement noise variance. In the case of low measurement noise variance, increasing the total available power P_T results in channel inversion being asymptotically optimal, as is suggested by (19) wherein the first term dominates.

C. Numerical Results

From (16), we see that the number of active sensors depends on the distribution of the channel SNRs and the measurement noise variances. These simulations use $K = 500$ sensors and channel SNRs $r_i \sim U[0, 25]$ dB. The channel SNRs are randomly generated, but once selected, they are fixed and known at the fusion center. Let R be any positive random variable, and as in [3], define

$$\text{normalized deviation of } R, \tilde{R} = \frac{\sqrt{\text{var}(R)}}{\mathbb{E}(R)} \quad (21)$$

which is used as a measure of heterogeneity of R . For $r \sim U[a, b]$, we have $\tilde{r} = (b-a)/[\sqrt{3}(b+a)]$. The number of active sensors is computed using (16) for the equal measurement noise variance case, and the results are averaged over 100 realizations of the channel gains.

The effect that increasing the measurement noise variance has on the percentage of active sensors is shown in Fig. 3 for three values of \tilde{R} . As expected from the discussion in the previous subsection, a larger measurement noise variance requires a higher percentage of active sensors. Since only ‘‘imperfect’’ measurements are available, a greater number of observations are needed to average out the effects of the measurement noise. Also notice for a fixed σ_z^2 , that as \tilde{R} increases, the percentage of active sensors *decreases*. A higher \tilde{R} value corresponds to a greater diversity in channel SNRs, so the optimal power allocation strategy selects sensors with better SNRs, resulting in a smaller number of active sensors.

IV. THE BRANCH TOPOLOGY

A. Deriving the MSE Expressions

We now focus on a generalization of the star topology, i.e., the branch topology. The generic branch topology consists of N leaf nodes connected to the fusion center via a single relay connected to all nodes, as shown in Fig. 1(b). Measurements are taken at all nodes and transmitted to the fusion center using either the AF or EF protocol. As stated earlier, the time resources utilized to form the estimate at the fusion center in the branch topology are the same for both AF and EF protocols.¹⁰

For the amplify-and-forward case, the fusion center receives $N + 1$ measurements, which are given by

$$y_0 = \sqrt{\frac{P_0}{N+1}} h_0 \beta(z_0) (\theta + z_0) + n_0 \quad (22)$$

$$y_i = \sqrt{\frac{P_0}{N+1}} h_0 \gamma(P_i) [\sqrt{P_i} h_i \beta(z_i) (\theta + z_i) + n_i] + n_{0i} \quad (23)$$

for $i = 1, \dots, N$, from the relay node and the N leaf nodes, respectively. As before, we assume that equal powers are used to forward each of the $N + 1$ measurements from the relay node to the fusion center. The fusion center forms the optimal BLU estimate, for which we derive the corresponding MSE as

$$\text{MSE}_{\text{branch,AF}} = \left(\frac{1}{\sigma_{z_0}^2 + \frac{1}{r_0 P_0 \beta^2(z_0)}} + \sum_{i=1}^N \frac{1}{\sigma_{z_i}^2 + \frac{1}{r_i P_i \beta^2(z_i)} \left(1 + \frac{N+1}{r_0 P_0 \gamma^2(P_i)} \right)} \right)^{-1} \quad (24)$$

In the case of estimate-and-forward, the relay node receives $N + 1$ measurements, given by

$$y_0 = \theta + z_0 \quad (25)$$

$$y_i = \sqrt{P_i} h_i \beta(z_i) (\theta + z_i) + n_i, \quad i = 1, \dots, N. \quad (26)$$

The relay estimates $\hat{\theta}_R$ and transmits this single measurement to the fusion center, which receives

$$y = \sqrt{P_0} h_0 \beta(n_R) (\theta + n_R) + n_0 \quad (27)$$

and computes the final estimate $\hat{\theta}_{\text{FC}}$ with an estimation error given by

$$\text{MSE}_{\text{branch,EF}} = \frac{1}{r_0 P_0 \beta^2(n_R)} + \sigma_{n_R}^2 \quad (28)$$

where

$$\sigma_{n_R}^2 = \left(\frac{1}{\sigma_{z_0}^2} + \sum_{i=1}^N \frac{1}{\sigma_{z_i}^2 + \frac{1}{r_i P_i \beta^2(z_i)}} \right)^{-1}.$$

¹⁰Since we have assumed that sensors communicate time-orthogonally within each level, both protocols require $N + 1$ transmission slots in order to send N measurements from the leaf nodes to the relay node, and then to the fusion center.

The minimization of the MSE expressions in (24) and (28) under a total network power constraint cannot be solved analytically. Since only numerical solutions are available, we next derive an upper bound which is asymptotically optimal for increasing measurement noise variance.

B. Asymptotic Analysis of the Branch Topology

Recall the arithmetic mean—harmonic mean (AM-HM) inequality [22], which can be expressed as

$$\frac{1}{N^2}(x_1 + \dots + x_N) \geq \left(\frac{1}{x_1} + \dots + \frac{1}{x_N} \right)^{-1}. \quad (29)$$

For the simplified case with equal measurement noise variances for all nodes, applying (29) to the MSE expression in (24) yields¹¹

$$\begin{aligned} \overline{\text{MSE}}_{\text{branch,AF}} &= \frac{\sigma_z^2}{N+1} + \frac{1}{(N+1)^2} \left[\frac{N+1}{r_0 P_0 \beta^2(z_0)} \right. \\ &\quad \left. + \sum_{i=1}^N \frac{1}{r_i P_i \beta^2(z_i)} \left(1 + \frac{N+1}{r_0 P_0 \beta^2(P_i)} \right) \right]. \end{aligned} \quad (30)$$

Substituting (5) for $\beta^2(P_i)$ into (30) and rewriting the upper bound yields

$$\overline{\text{MSE}}_{\text{branch,AF}} = S + \sum_{i=1}^N \frac{1}{t_i P_i} \quad (31)$$

where

$$t_i = (N+1)^2 r_i \beta^2(z_i) \left(1 + \frac{(N+1)\sigma_{n_i}^2}{r_0 P_0} \right)^{-1} \quad (32)$$

and

$$S = \frac{\sigma_z^2}{N+1} + \frac{1}{(N+1)^2} \left[\frac{N+1}{r_0 P_0 \beta^2(z_0)} + \frac{N+1}{r_0 P_0} \sum_{i=1}^N \frac{\sigma_{n_i}^2}{\beta^2(z_i)} \right] \quad (33)$$

to illustrate the dependence of $\overline{\text{MSE}}_{\text{branch,AF}}$ on the leaf node powers $\{P_i\}_{i=1}^N$. As an aside, consider the optimization problem

$$\text{minimize } \sum_{i=1}^N \frac{1}{a_i x_i} \quad \text{subject to } \sum_{i=1}^N x_i = x_T \quad (34)$$

which is optimized by $x_i^* = 1/\sqrt{a_i \nu^*}$ where $\nu^* = (\sum_{i=1}^N 1/\sqrt{x_i})^2$ is the optimal value of the Lagrange multiplier associated with the power constraint. Applying this result to the AF upper bound, we obtain

$$\overline{P}_i^* = \frac{\alpha_t}{\sqrt{t_i}} \left(P_T - \overline{P}_0^* \right) \quad \text{with } \alpha_t = \left(\sum_{j=1}^N \frac{1}{\sqrt{t_j}} \right)^{-1} \quad (35)$$

¹¹We denote the upper bound for the MSE as $\overline{\text{MSE}}$, and thus it is always the case that $\text{MSE} \leq \overline{\text{MSE}}$.

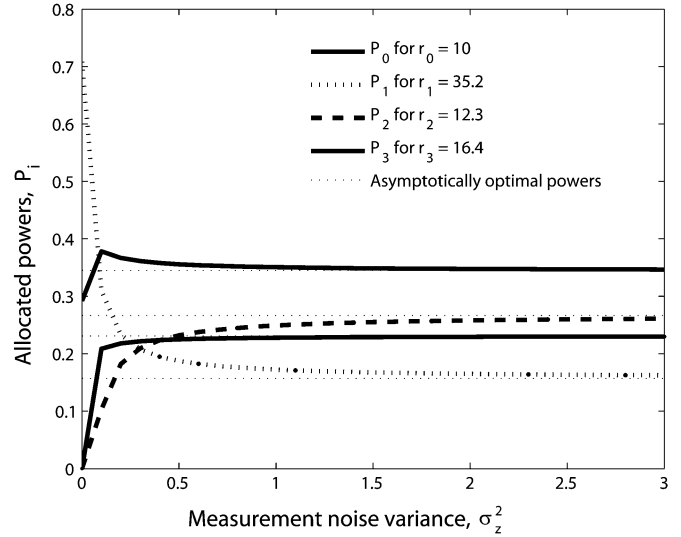


Fig. 4. Optimal and asymptotically optimal powers for the branch topology.

which minimizes (30), and where t_i is given in (36). Thus, the optimal power allocated to the relay node can be computed as the result of a one-variable numerical optimization. Similarly, the corresponding upper bound for the branch EF case is given by

$$\begin{aligned} \overline{\text{MSE}}_{\text{branch,EF}} &= \frac{\sigma_\theta^2}{r_0 P_0} + \left(1 + \frac{1}{r_0 P_0} \right) \frac{1}{(N+1)^2} \\ &\quad \times \left[(N+1)\sigma_z^2 + (\sigma_\theta^2 + \sigma_z^2) \sum_{i=1}^N \frac{1}{r_i P_i} \right] \end{aligned} \quad (36)$$

which has the optimal limiting powers for the leaf nodes given by (35) with $t_i = r_i$, and whose relay node optimal power can also be computed numerically. In both the AF and EF cases, the optimal limiting power allocated to the leaf nodes corresponds to channel inversion.

This optimal limiting power allocation scheme is intuitive. Since the relay node is utilized by all the leaf nodes to forward measurements to the fusion center, \overline{P}_0^* is not a function of any one of the individual leaf node SNRs. On the other hand, the optimal limiting leaf node powers are allocated using channel inversion since the leaf nodes resemble a star topology with respect to the relay node. Sensors with weaker SNRs are allocated a greater fraction of the remaining power $P_T - \overline{P}_0^*$.

The upper bound for the branch topology, as well as for the tree and linear topologies, is tight for modest values of σ_z^2 , as shown in Fig. 4. The bold lines represent the optimal powers allocated to the relay P_0 , and the three leaf nodes $\{P_1, P_2, P_3\}$, and the regular dotted lines represent their respective asymptotically optimal powers. The optimal powers allocated to the nodes are nearly equal to those computed using the upper bound for $\sigma_z^2 > 1.5$, but the upper bound is clearly ineffective when $\sigma_z^2 \approx 0$ and sensor selection is optimal. Thus, these bounds are useful analytic solutions in the case of moderate to high measurement noise, and a viable alternative to purely numerical solutions for many practical scenarios.

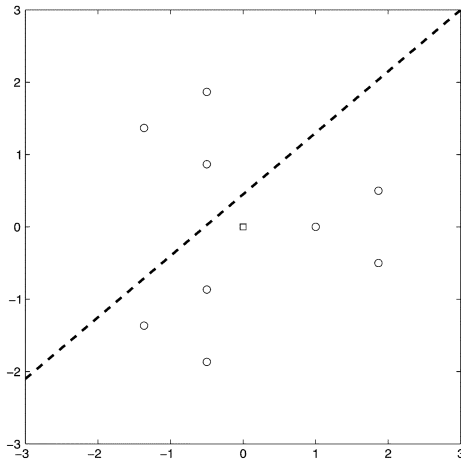


Fig. 5. Tree topology and trajectory.

V. THE TREE TOPOLOGY

A. Algorithm for Optimal Power Allocation

The single branch topology can be arbitrarily replicated to form a generic “one-layer” tree topology. Assume that there are K relaying nodes connected to the fusion center, and that each relaying node has N_k leaf nodes attached to the k th relay node. The MSE for the tree topology can be computed as

$$\text{MSE}_{\text{tree,AF/EF}} = \left(\sum_{k=1}^K \frac{1}{\text{MSE}_{\text{branch,AF/EF}}^k} \right)^{-1} \quad (37)$$

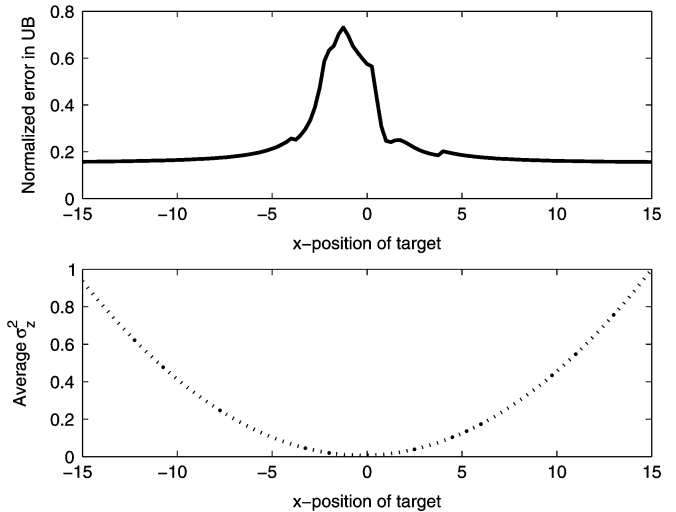
which suggests that the MSE for the entire tree can be minimized by independently minimizing the estimation error for each of the individual branches, each of which operates under its own sum power constraint. The asymptotically optimal power policy for the AF/EF branch case can directly be used to obtain the optimal limiting power allocation for the one-layer tree topology. In particular, an algorithm for the asymptotically optimal power allocation is outlined as follows.

- 1) Assign dummy total powers to each of the branches $P_{T,i}, i = 1, \dots, K$
- 2) Each branch is optimized by the optimal limiting power allocations described in the previous section, but using a sum power constraint of $P_{T,i}$.
- 3) The resulting MSE_{tree} can now be optimized over the set of total powers for each branch $\{P_{T,i}\}_{i=1}^K$.

Analytic solutions for the tree topology are unavailable because step (3) requires a numerical optimization. This algorithm highlights the fact that the optimal powers assigned to the branches of a tree are simply scaled versions of the single branch optimal powers. In particular, channel inversion is used to optimally allocate leaf node powers to ensure that all measurements are useful at the fusion center.

B. Numerical Results

Consider a symmetric tree topology with $K = 3, N_k = 2 \forall k$, wherein the MSE of the parameter estimate at the fusion center is minimized for a source placed at different locations on the dashed line, shown in Fig. 5 for the x -coordinate $\in [-15, 15]$. Note that “target tracking” is not considered here. Rather, the

Fig. 6. MSE error and variance in σ_z^2 for target with $C = 0.5$.

transmission power is optimized to reduce the estimation error at the fusion center at each source location on the trajectory.¹² Since the distances between the leaf and relay nodes and the relay nodes and the fusion center are the same, the channel SNR r is assumed to be constant for all links. The measurement noise variance at the leaf and relay nodes is modeled as a function of the distance between that node and a point on the trajectory, i.e.,

$$\sigma_z^2 = Cd^2 \quad (38)$$

where C is arbitrarily chosen to vary the dependence of the measurement noise on the distance parameter. Thus, the measurement noise varies with changing target location. The error in the upper bound of the MSE for the tree topology (the upper plot) and the corresponding average measurement noise variance (the lower plot) are shown in Fig. 6 for $r = 10$ dB, $C = 0.5$. We see in this figure that the upper bound of the MSE is tight for moderate and large values of the measurement noise variance. In fact, the error between the upper bound and the optimal solution increases only when $\sigma_z^2 \approx 0$. Thus, the asymptotically optimal solution derived for increasing σ_z^2 is tight even for modest values of the measurement noise variance.

VI. POWER ALLOCATION IN LINEAR TOPOLOGIES

The two-hop linear topology is shown in Fig. 1(c). In the N -hop topology, we assume for both AF and EF protocols that measurements are made at both the leaf and $N - 1$ relay nodes.

A. Problem Formulation for the AF Protocol

Since a relay node equally divides the power allocated to it among the measurements forwarded through it, as well as its own measurement, the N received signals at the fusion center are given by

$$y_1 = \sqrt{\frac{P_1}{N}} h_1 \beta(z_1) (\theta + z_1) + n_1 \quad (39)$$

¹²As seen in Fig. 5, the track is not perfectly symmetric with respect to the fusion center, and thus, the maximum error in the upper bound (in the upper plot of Fig. 6) does not occur at $x = 0$.

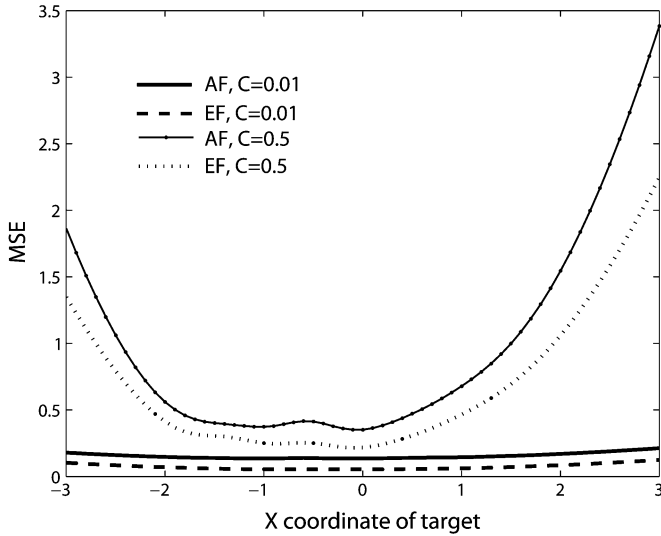


Fig. 7. MSE for EF and AF protocols.

$$y_2 = \sqrt{\frac{P_1}{N}} h_1 \gamma \left(\frac{P_2}{N-1} \right) \left(\sqrt{\frac{P_2}{N-1}} h_2 \beta(z_2) (\theta + z_2) + n_2 \right) + n_1$$

$$\vdots \quad (40)$$

$$y_N = \sqrt{\frac{P_1}{N}} h_1 \gamma \left(\frac{P_2}{N-1} \right) (\dots \gamma(P_N) \times (\sqrt{P_N} h_N \beta(z_N) (\theta + z_N) + n_N) \dots) + n_1 \quad (41)$$

which are used to compute the BLU estimate $\hat{\theta}$, with an estimation error derived as

$$\text{MSE}_{\text{linear,AF}} = \left(\frac{1}{\sigma_{z_1}^2 + \frac{N}{r_1 P_1 \beta^2(z_1)}} + \frac{1}{\sigma_{z_2}^2 + \frac{N-1}{r_2 P_2 \beta^2(z_2)} \left(1 + \frac{N}{r_1 P_1 \gamma^2(P_2)} \right)} + \dots \right)^{-1} \quad (42)$$

In this linear AF case, the optimal power allocation policy is obtained using numerical optimization techniques. Even an analytic solution, in the asymptotic $\sigma_z^2 \rightarrow \infty$ limit, appears intractable since the power variables are nonseparable. However, for estimate-and-forward, we can determine closed form solutions for optimizing the limiting MSE.

B. Problem Formulation and Solution for the EF Protocol

Using the EF protocol, each relay node combines two measurements to compute $\hat{\theta}_R$: the one made at that relay node and the one received from the previous node. Finally, the fusion center computes a BLU estimate, with the corresponding MSE given recursively as

$$\text{MSE}_{\text{linear,EF}} = \frac{1}{r_1 P_1 \beta^2(\bar{z}_1)} + \sigma_{\bar{z}_1}^2 \quad (43)$$

where

$$\sigma_{\bar{z}_i}^2 = \left(\frac{1}{\sigma_{z_i}^2} + \frac{1}{\sigma_{z_{i+1}}^2 + \frac{1}{r_{i+1} P_{i+1} \beta^2(\bar{z}_{i+1})}} \right)^{-1} \quad (44)$$

for $i = 1, \dots, N-1$, and $\sigma_{\bar{z}_N}^2 = \sigma_{z_N}^2$. In this case, the optimization problem can only be solved numerically. As in the branch topology, we develop intuition by considering the limiting minimization problem wherein the optimal solution is a weighted channel inversion type solution. Because the variables are nonseparable, the asymptotic solution is difficult and awkward to characterize for the general N sensor linear EF case. Thus, we further consider the limit $P_T \rightarrow \infty$. For increasing P_T , the upper bound on the MSE expression can be written as

$$\lim_{\sigma_z^2 \rightarrow \infty} \lim_{P_T \uparrow} \text{MSE}_{\text{linear,EF}} = \sum_{i=1}^N \frac{1}{c_i^2 r_i P_i} \quad (45)$$

where $c_i = N/(N-i+1)$. Note that the asymptotically optimal power allocation strategy (for increasing P_T) is given by

$$P_i^* = \frac{\alpha}{\sqrt{c_i^2 r_i}} \quad \text{where} \quad \alpha = \left(\sum_{k=1}^N \frac{1}{\sqrt{c_k^2 r_k}} \right)^{-1} \quad (46)$$

which is a weighted channel inversion solution, and where c_i represents the position of that particular sensor with respect to the fusion center. Nodes closer to the fusion center are given “more weight,” as is indicated by $1/c_i^2$ in (45). Further note that, in the case of low measurement noise, sensors further away from the fusion center remain inactive to minimize the MSE.

VII. NUMERICAL RESULTS

Reconsider the symmetric tree topology shown in Fig. 5. To compare the amplify-and-forward protocol to the estimate-and-forward protocol, we choose parameters $r = 10$ dB and $C = 0.5, 0.01$. The MSE and number of active sensors as a function of the target x -axis position for the AF and EF protocols are shown in Figs. 7 and 8, respectively. Notice that the EF protocol consistently outperforms the AF case in this particular simulation, and the difference is relatively constant for both cases of the measurement noise variance. This is so because the propagation of the channel noise, given the simulation parameters, affects the MSE at the fusion center to a greater extent than the estimation errors at the relay nodes. Note that we do not claim EF outperforms AF under all circumstances; merely that it does so for the case under examination in this paper. An overlay of Figs. 7 and 8 shows that, for the $C = 0.5$ case, the minimum MSE is achieved via sensor selection for both protocols when the measurement noise variance is low. In the $C = 0.01$ case, $\sigma_z^2 \approx 0$, and, thus, sensor selection is always optimal as reflected in Fig. 8.

Now consider different topologies imposed on a common set of nodes, as shown in Fig. 9. The EF protocol is used to compare the linear, branch, and “mixed” topologies for increasing measurement noise variance. The “mixed” topology is simply a two-level branch that incorporates features of both the linear

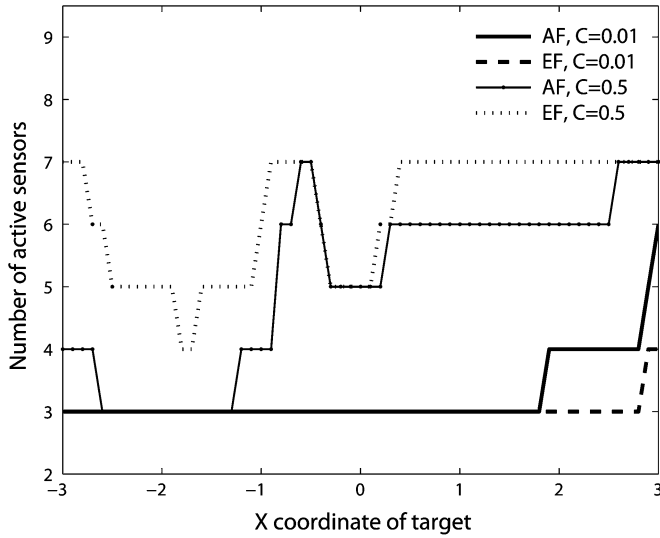


Fig. 8. Number of active sensors for EF and AF protocols.

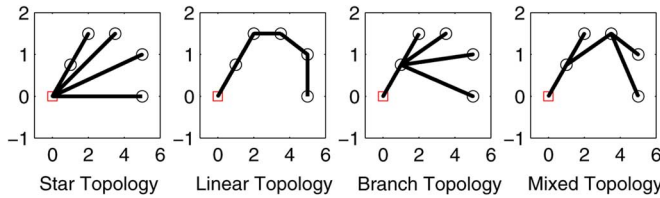


Fig. 9. Star, linear, branch, and mixed topologies imposed on the same set of nodes.

and branch topologies. Note that we assume σ_z^2 is equal for all the nodes, and that the channel SNR is given by

$$r_i = C d_i^{-\alpha} \quad (47)$$

where d_i is the distance between adjacent communicating nodes, C is an arbitrary constant that varies the dependence of the SNR on the distance, and we assume $\alpha = 2$ is the path-loss exponent. For $C = 20$,¹³ we find that

$$\text{MSE}_{\text{Mixed}} < \text{MSE}_{\text{Branch}} < \text{MSE}_{\text{Star}} < \text{MSE}_{\text{Linear}} \quad (48)$$

for all values of $\sigma_z^2 > 0$. The linear topology yields the highest optimal MSE, and the minimum MSE decreases as the depth of branching increases. The increased branching results in the transmission of measurements over shorter distances and greater data fusion at the relay nodes. Fig. 10 compares the MSE for these topologies, in the high measurement noise variance case, as the path-loss exponent $\alpha \in [2, 4]$ varies. We see that the linear topology, with shorter hops, yields a lower MSE than both the branch and star topologies as the attenuation due to distance increases. However, the mixed topology yields the lowest MSE $\forall \alpha$, and thus more hierarchical networks appear to be preferable for the constant measurement noise variance case.

¹³The C value for this simulation is significantly larger because we require all sensors to be active for the topology comparison.

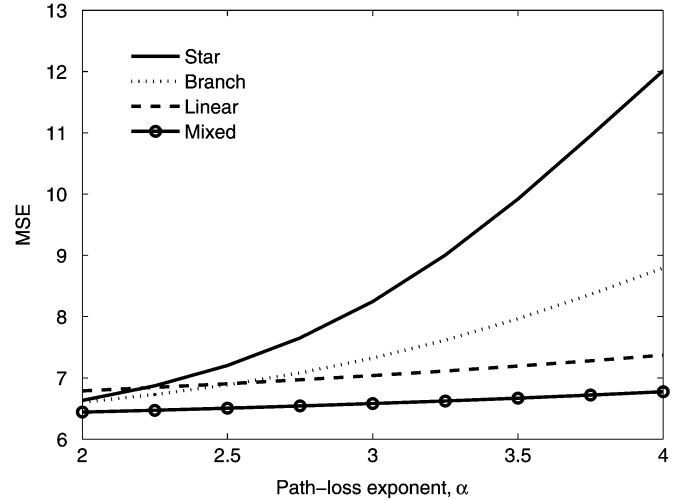


Fig. 10. MSE of different topologies for varying α .

VIII. CONCLUSION

A power allocation problem for parameter estimation with distributed observations under a total network power constraint was considered for various topologies. An analysis of the star topology was presented which noted that the measurement noise variance changes the nature of the optimal solution. For $\sigma_z^2 \approx 0$, sensor selection is optimal, but as σ_z^2 increases, the solution evolves from waterfilling to channel inversion. If only noisier measurements are available, the fusion center uses all the sensors to obtain a better estimate, and to this end, sensors with lower SNRs are allocated a greater fraction of the total power (channel inversion).

A similar solution space is derived for the leaf nodes of the branch topology, but this is observed only when an alternate optimization problem is solved. An upper bound is obtained for the MSE that is asymptotically equal to the true MSE in the limit of large measurement noise. This approach allows us to derive the optimal power allocation for complex topologies whose exact MSEs can only be solved numerically. For the scenarios we have examined, we see that the optimization of the limiting MSE results in a power allocation that is near optimal even for modest measurement noise. The single branch topology is easily extended to the generic one-layered tree topology, which, though it requires some numerical optimization, exhibits a channel inversion limiting power allocation for the leaf nodes of each branch. For common values of the path-loss exponent, hierarchical networks yield the lowest MSE for the equal measurement noise variance case.

Future work includes investigating the performance of the EF and AF protocols for different and more generic topologies, and for varying values of C . Power allocation schemes that do not require perfect knowledge of the channel gains at the fusion center are also of further interest.

APPENDIX I

NOTE ON ORTHOGONAL COMMUNICATION

In the orthogonal communication case, the fusion center receives the following N measurements from the sensors¹⁴

$$y_i = \sqrt{P_i}h_i(\theta + z_i) + n_i, \quad i = 1, \dots, N. \quad (49)$$

The BLU estimate computed at the fusion center has a corresponding estimation error given by

$$\text{MSE}_{\text{orthogonal}} = \left(\sum_{i=1}^N \frac{1}{\sigma_i^2 + \frac{1}{r_i P_i}} \right)^{-1}. \quad (50)$$

Minimizing the MSE shown above subject to a total network power constraint $\sum_{i=1}^N P_i = P_T$ yields the optimal power allocation policy

$$P_i^* = \frac{1}{r_i \sigma_i^2} \left(\sqrt{\frac{r_i}{\nu^*}} - 1 \right)^+ \quad (51)$$

where ν^* is the optimal value of the Lagrange multiplier. Assume that all the measurement noise variances are equal, and compute the minimum MSE as

$$\begin{aligned} \text{MSE}_{\text{orthogonal}}^* &= \sigma_z^2 \left(P_T \sigma_z^2 + \sum_{i=1}^{N'} \frac{1}{r_i} \right) \\ &\times \left[N' P_T \sigma_z^2 + N' \sum_{i=1}^{N'} \frac{1}{r_i} - \left(\sum_{i=1}^{N'} \frac{1}{\sqrt{r_i}} \right)^2 \right]^{-1} \end{aligned} \quad (52)$$

where N' is the number of active sensors.

On the other hand, in the parallel communication case, the fusion center receives a single measurement given by

$$y = (\sqrt{P_1}h_1 + \dots + \sqrt{P_N}h_N)(\theta + z) + n \quad (53)$$

and the BLUE MSE is derived as

$$\text{MSE}_{\text{parallel}} = \bar{\sigma}_z^2 + \frac{\bar{\sigma}_n^2}{(\sqrt{P_1}h_1 + \dots + \sqrt{P_N}h_N)^2}. \quad (54)$$

The optimal power allocation policy in the parallel communication case is

$$P_i^* = \frac{h_i^2}{4} \left(\sum_{k=1}^N \frac{h_k^2}{4} \right)^{-1} P_T. \quad (55)$$

Thus, we can rewrite the minimum MSE as

$$\begin{aligned} \text{MSE}_{\text{parallel}}^* &= \bar{\sigma}_z^2 + \bar{\sigma}_n^2 \left[P_T \sum_{i=1}^N h_i^2 \right]^{-1} \\ &= N \sigma_z^2 + N \left(P_T \sum_{i=1}^N r_i \right)^{-1} \end{aligned} \quad (56)$$

¹⁴Since the orthogonal communication aspect is not analyzed asymptotically (for increasing σ_z^2), the normalization functions $\beta(\cdot)$ and $\gamma(\cdot)$ have been omitted from the signal model to simplify the analysis.

where we have assumed the measurement and channel noise variances for the single measurement are equal to the sum of the noise variances from the orthogonal case.

For low measurement noise variance, sensor selection is optimal in the orthogonal communication case. Thus, comparing the analytical MSE expressions is difficult, but numerical simulations indicate that $\text{MSE}_{\text{orthogonal}}$ is smaller. In the limit $\sigma_z^2 \rightarrow \infty$, all the sensors are active, i.e., $N' = N$, and we can compute

$$\begin{aligned} \overline{\text{MSE}}_{\text{orthogonal}} &= \frac{\sigma_z^2}{N} \\ \overline{\text{MSE}}_{\text{parallel}} &= \bar{\sigma}_z^2 = N \sigma_z^2. \end{aligned}$$

The orthogonal communication MSE is lower than the parallel case, even if we assume that the single measurement in the parallel case has measurement noise variance σ_z^2 instead of $N \sigma_z^2$.

APPENDIX II

SIGNAL MODEL EXTENSIONS

A. Multipath Channel Model

Multipath models exist for several environments of interest, such as wireless and underwater channels [24]. We show here that multipath is easily accommodated in our framework. A multipath channel with known channel attenuation coefficients at the fusion center is considered. Assume that each sensor in a star topology sends a single measurement (corrupted by measurement noise) to the fusion center over L multipath fingers. From each sensor, the fusion center receives the observation

$$\underline{x}_i = \sqrt{P_i} \underline{h}_i \beta(z_i)(\theta + z_i) + \underline{n}_i \quad (57)$$

where the generic vector \underline{a}_i is defined as $[a_{i1}, a_{i2}, \dots, a_{iL}]^T$, and $\underline{x}_i, \underline{h}_i$ and \underline{n}_i represent the received signals, channel attenuation coefficients, and channel noises of the i th sensor, respectively. Note that h_{ij} represents the channel attenuation coefficient of the j th path for the i th sensor.

The fusion center has all NL observations available and constructs the $NL \times 1$ vector

$$\underline{X} = [\underline{x}_1, \underline{x}_2, \dots, \underline{x}_N]^T \quad (58)$$

where \underline{x}_i is as defined in (57). A RAKE receiver [16] is implemented at the fusion center that computes the sufficient statistic $\tilde{\underline{x}} = \mathbf{H}\underline{X}$ using the $N \times NL$ block-diagonal channel matrix $\mathbf{H} = \text{diag}(\underline{h}_1, \underline{h}_2, \dots, \underline{h}_N)$.

The output of the RAKE receiver is

$$\tilde{x}_i = \sqrt{P_i} \|\underline{h}_i\|^2 \beta(z_i)(\theta + z_i) + \sum_{j=1}^L h_{ij} n_{ij} \quad (59)$$

for $i = 1, \dots, N$, which is now used to compute the BLUE and corresponding MSE. Equation (59) can be rewritten as

$$\tilde{x}_i = \sqrt{P_i} \|\underline{h}_i\|^2 \beta(z_i)\theta + w_i \quad (60)$$

where

$$\sigma_{w_i}^2 = \|\underline{h}_i\|^2 (P_i \|\underline{h}_i\|^2 \beta(z_i) \sigma_{z_i}^2 + \sigma_{n_i}^2) \quad (61)$$

if we assume that the channel noise is independent for each multipath finger. The MSE corresponding to the best linear unbiased estimate is computed as

$$\text{MSE}_{\text{MP}} = \sum_{i=1}^K \frac{P_i \|\underline{h}_i\|^2 \beta^2(z_i)}{P_i \|\underline{h}_i\|^2 \beta^2(z_i) \sigma_{z_i}^2 + \sigma_{n_i}^2}. \quad (62)$$

Compare this to the original MSE in the “single path” case,

$$\text{MSE}_{\text{SP}} = \sum_{i=1}^K \frac{P_i h_i^2 \beta^2(z_i)}{P_i h_i^2 \beta^2(z_i) \sigma_{z_i}^2 + \sigma_{n_i}^2}. \quad (63)$$

We find that we can simply replace h_i^2 by $\|\underline{h}_i\|^2$, given the noise and channel state information assumptions. Thus, the optimal power allocation solution is still given by (17), but now $r_i = \|\underline{h}_i\|^2 / \sigma_{n_i}^2$. Note that these results also hold for the other more complex topologies considered.

B. Vector Parameter Estimation

Vector estimation in the more complicated topologies has several real-world applications. The scalar parameter estimation framework presented in this work can easily be extended to the estimation of a vector of distinct independent parameters. Note that the deterministic channel from the node to the fusion center is the same for all sensors at that particular node. Given the star topology, we assume N nodes, each with M sensors, and thus the fusion center receives $N \times M$ measurements given by

$$y_{ij} = \sqrt{P_{ij}} h_i \beta(z_{ij}) (\theta_j + z_{ij}) + n_{ij} \quad (64)$$

for $i = 1, \dots, N$ and $j = 1, \dots, M$.

In the case that all the measurement noise and channel noise terms are independent, the BLU estimate at the fusion center has a corresponding estimation error given by

$$\begin{aligned} \text{MSE} &= \sum_{j=1}^M \left[\left(\sum_{i=1}^N \frac{1}{\sigma_{z_{ij}}^2 + \frac{\sigma_{n_{ij}}^2}{P_{ij} |h_i|^2 \beta^2(z_{ij})}} \right)^{-1} \right] \\ &= \sum_{j=1}^M \text{MSE}_{j^{\text{th}} \text{ parameter}}. \end{aligned} \quad (65)$$

Thus, the MSE at the fusion center for vector parameter estimation is simply the sum of the MSEs for each of the M independent parameters¹⁵ (with a nonseparable total network power constraint). An algorithm similar to the one used to solve the one-layer tree topology may be employed here.

ACKNOWLEDGMENT

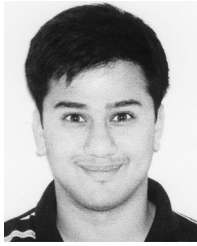
The authors would like to thank Prof. F. Ordonez of the USC Department of Industrial and Systems Engineering for his time and suggestions during the development of this paper.

¹⁵In the case of correlated parameters, the MSE at the fusion center can only be expressed in matrix notation with a nondiagonal covariance matrix, and yields a more complicated expression than the sum of the individual MSEs.

REFERENCES

- [1] W. Li and C. G. Cassandras, “A minimum-power wireless sensor network self-deployment scheme,” presented at the 2005 IEEE Wireless Commun. Netw. Conf. (WCNC), New Orleans, LA, Mar. 2005.
- [2] V. Delouille, R. Neelamani, and R. Baraniuk, “Robust distributed estimation in sensor networks using the embedded polygons algorithm,” presented at the 3rd Int. Conf. Inf. Process. Sensor Netw. (IPSN), Los Angeles, CA, Apr. 2004.
- [3] J.-J. Xiao, S. Cui, Z.-Q. Luo, and A. J. Goldsmith, “Power scheduling of universal decentralized estimation in sensor networks,” *IEEE Trans. Signal Process.*, vol. 54, no. 3, pp. 1131–1143, Mar. 2006.
- [4] S. Cui, J. Xiao, A. J. Goldsmith, Z.-Q. Luo, and H. V. Poor, “Estimation diversity and energy efficiency in distributed sensing,” *IEEE Trans. Signal Process.*, vol. 55, no. 9, pp. 4683–4695, Sep. 2007.
- [5] S.-H. Son, M. Chiang, S. R. Kulkarni, and S. C. Schwartz, “The value of clustering in distributed estimation for sensor networks,” in *Proc. 2005 Int. Conf. Wireless Netw., Commun. Mobile Computing*, Jun. 2005, vol. 2, pp. 969–974.
- [6] X. Wu and Z. Tian, “Optimized data fusion in bandwidth and energy constrained sensor networks,” in *Proc. IEEE Int. Conf. Acoust., Speech, Signal Process.*, May 2006, vol. 4, pp. IV–713, IV–716.
- [7] Z.-Q. Luo, “Universal decentralized estimation in a bandwidth constrained sensor network,” *IEEE Trans. Inf. Theory*, vol. 51, no. 6, pp. 2210–2219, Jun. 2005.
- [8] A. Ribeiro and G. B. Giannakis, “Bandwidth-constrained distributed estimation for wireless sensor networks-Part I: Gaussian case,” *IEEE Trans. Signal Process.*, vol. 54, no. 3, pp. 1131–1143, Mar. 2006.
- [9] R. Nowak, U. Mitra, and R. Willett, “Estimating inhomogeneous fields using wireless sensor networks,” *IEEE J. Sel. Areas Commun.*, vol. 22, pp. 999–1006, Aug. 2004.
- [10] R. Pon, M. Batalin, J. Gordon, A. Kansal, D. Liu, M. Rahimi, L. Shirachi, Y. Yu, M. Hansen, W. Kaiser, M. Srivastava, G. Sukhatme, and D. Estrin, “Networked infomechanical systems: A mobile embedded networked sensor platform,” presented at the Int. Conf. Inf. Process. Sensor Netw. (IPSN), Los Angeles, CA, Apr. 2005.
- [11] B. Zhang and G. Sukhatme, “Adaptive sampling for estimating a scalar field using a robotic boat and a sensor network,” presented at the IEEE Int. Conf. Robot. Autom. (ICRA), Rome, Italy, Apr. 2007.
- [12] N. Ramanathan, L. Balzano, D. Estrin, M. Hansen, T. Harmon, J. Jay, W. Kaiser, and G. Sukhatme, “Designing wireless sensor networks as a shared resource for sustainable development,” presented at the 1st Int. Conf. Inf. Commun. Technol. Develop., Berkeley, CA, May 2006.
- [13] S.-H. Son, S. R. Kulkarni, S. C. Schwartz, and M. Roan, “Communication-estimation tradeoffs in wireless sensor networks,” presented at the IEEE Int. Conf. Acoust., Speech, Signal Process. (ICASSP), Philadelphia, PA, Mar. 2005.
- [14] M. Chu, H. Haussecker, and F. Zhao, “Scalable information-driven sensor querying and routing for ad hoc heterogeneous sensor networks,” *Int. J. High Perform. Computing Applicat.*, vol. 16, no. 3, pp. 90–110, Aug. 2002.
- [15] G. Thattai and U. Mitra, “Power allocation in linear and tree WSN topologies,” presented at the 40th Asilomar Conf. Signals, Syst. Comput., Asilomar, CA, Oct. 2006, Invited Paper.
- [16] D. Tse and P. Viswanath, *Fundamentals of Wireless Communications*. New York: Cambridge Univ. Press, 2005.
- [17] G. Caire and U. Mitra, “Structured multiuser channel estimation for block-synchronous DS/CDMA,” *IEEE Trans. Commun.*, vol. 49, no. 9, pp. 1605–1617, Sep. 2001.
- [18] S. M. Kay, *Fundamentals of Statistical Signal Processing: Estimation Theory*. Englewood Cliffs, NJ: Prentice-Hall, 1993.
- [19] S. Vedantam, U. Mitra, and A. Sabharwal, “Shared sensing and communications in sensor networks: The multihop case,” presented at the IEEE Int. Symp. Inf. Theory (ISIT), Seattle, WA, Jul. 2006.
- [20] S. Boyd and L. Vandenberghe, *Convex Optimization*. Cambridge, U.K.: Cambridge Univ. Press, 2004.
- [21] A. Lozano, A. Tulino, and S. Verdú, “Mercury/waterfilling: Optimum power allocation with arbitrary input constellations,” presented at the IEEE Int. Symp. Inf. Theory (ISIT), Adelaide, Australia, Sep. 2005.
- [22] M. Abramowitz and I. A. Stegun, *Handbook of Mathematical Functions with Formulas, Graphs, and Mathematical Tables*. New York: Dover, 1964.
- [23] R. Fourer, D. M. Gay, and B. W. Kernighan, *AMPL: A Modeling Language for Mathematical Programming*. Pacific Grove, CA: Duxbury, 2002.

- [24] M. Stojanovic, "Recent advances in high-speed underwater acoustic communications," *IEEE J. Ocean. Eng.*, vol. 21, no. 2, pp. 125–136, Apr. 1996.



Gautam Thatte (S'05) was born in Bombay, India, in 1981. He received the B.S. degree (distinction) in engineering from Harvey Mudd College (HMC), Claremont, CA, in 2003 and the M.S. degree in electrical engineering from the University of Southern California (USC), Los Angeles, in 2004.

Currently, he is working toward the Ph.D. degree in electrical engineering at USC. His current research interests are in the areas of estimation and detection in sensor networks and computer networks.

Mr. Thatte is a member of Tau Beta Pi. He was awarded the USC Viterbi School of Engineering Dean's Fellowship and the HMC International Student Scholarship, in academic years 2003–2004 and 1999–2003, respectively.

Urbashi Mitra (F'07) received the B.S. and M.S. degrees from the University of California at Berkeley in 1987 and 1989, respectively, both in electrical en-

gineering and computer science. In 1994, she received the Ph.D. degree in electrical engineering from Princeton University, Princeton, NJ.

From 1989 until 1990, she was a Member of Technical Staff at Bellcore, Red Bank, NJ. From 1994 to 2000, she was a member of the faculty of the Department of Electrical Engineering, The Ohio State University, Columbus. In 2001, she joined the Department of Electrical Engineering, University of Southern California, Los Angeles, where she is currently a Professor.

Dr. Mitra is currently an Associate Editor for the *IEEE TRANSACTIONS ON INFORMATION THEORY* and the *IEEE JOURNAL OF OCEANIC ENGINEERING*. She was an Associate Editor for the *IEEE TRANSACTIONS ON COMMUNICATIONS* from 1996 to 2001. She is serving a second term as a member of the IEEE Information Theory Society's Board of Governors. She is the recipient of the Texas Instruments Visiting Professor (Fall 2002, Rice University), 2001 Okawa Foundation Award, 2000 Lumley Award for Research (OSU College of Engineering), 1997 MacQuigg Award for Teaching (OSU College of Engineering), 1996 National Science Foundation (NSF) CAREER Award, 1994 NSF International Postdoctoral Fellowship, 1998 Lockheed Leadership Fellowship, 1987 California Microelectronics Fellowship. She has co-chaired the IEEE Communication Theory Symposium at ICC 2003 in Anchorage, AK, and the first ACM Workshop on Underwater Networks at Mobicom 2006, Los Angeles, CA. She was the tutorials Chair for IEEE ISIT 2007 in Nice, France, and is currently the Finance Chair for IEEE ICASSP 2008 in Las Vegas, NV. She has held visiting appointments at: the Eurecom Institute, Rice University and Stanford University. She served as co-Director of the Communication Sciences Institute at the University of Southern California from 2004 to 2007.